6

High-Precision Three-Axis Force Sensor for Five-Fingered Haptic Interface

Takahiro Endo[1], Haruhisa Kawasaki[1], Kazumi Kouketsu[2]
and Tetsuya Mouri[1]
[1]*Gifu University*
[2]*Tec Gihan Co. LTD*
Japan

1. Introduction

Haptic interfaces that present force and tactile feeling have been utilized in the areas of telemanipulation (Ivanisevi & Lumelsky, 2000; Elhajj et al., 2001), interaction with micro/nano scale phenomena (Ando et al., 2001; Marliere et al., 2004), medical training and evaluation (Langrana et al., 1994; Basdogan et al., 2001), and so on. Haptic interfaces are key devices in constructing virtual reality environments. In contrast with single-point haptic interfaces, multi-fingered haptic interfaces hold promise for the above-mentioned applications and should dramatically increase the believability of the haptic experience (Magnenat-Thalmann & Bonanni, 2006). From these points of view, several multi-fingered haptic interfaces (Kawasaki & Hayashi, 1993; Ueda & Maeno, 2004; Walairacht et al., 2001; Bouzit et al., 2002; Adachi et al., 2002; Yoshikawa & Nagara, 2000; Immersion Corporation) have been developed.

A haptic interface consisting of an arm and fingertips (Adachi et al., 2002; Yoshikawa & Nagara, 2000; Immersion Corporation) can be used in a wide space. However, most of them consist of a hand and arm exoskeleton system. With this system, it is hard to represent the weight of virtual objects through the fingertips because the hand mechanism is mounted on the back of a human hand. Fixing the haptic interface to the hand binds the hand and creates an oppressive sensation in the operator. Moreover, the operator is subject to a strong sense of unease when the system performs abnormally. The haptic interface must be safe, function in a wide space, and represent not only the force at the contact points but also the weight of virtual objects. In addition, it should not cause an oppressive feeling when it attached to humans and should not represent its own weight. In order to solve these problems, we have developed a multi-fingered haptic interface robot, which is placed opposite to the human hand: HIRO (Kawasaki et al., 2003) and HIRO II+ (Kawasaki & Mouri, 2007). However, HIRO and HIRO II+ have high reduction mechanisms at all finger joints, an arrangement that ensures the compactness of the mechanism, but requires force sensors at the haptic fingertips.

Most haptic devices have a low reduction ratio, which permits impedance control without the use of a force sensor. However, this requires a large mechanism and entails difficulty in construction. Therefore, HIRO and HIRO II+ have high reduction mechanisms and require a

Source: Sensors, Focus on Tactile, Force and Stress Sensors, Book edited by: Jose Gerardo Rocha and Senentxu Lanceros-Mendez,
ISBN 978-953-7619-31-2, pp. 444, December 2008, I-Tech, Vienna, Austria

force sensor at each haptic fingertip. And, to accomplish high-precision force presentation to the operator, they require high-precision force sensors. From this point of view, we have developed high-precision three-axis force sensors and a compact sensor amplifier circuit with 15 channels. The developed force sensor uses strain gauges, and its diameter and length are 14 [mm] and 27 [mm], respectively. The size of the force sensor is small enough to install at the haptic fingertip. The force sensor signals are inputted to an interface FPGA circuit through a sensor amplifier circuit with a 24-bit A/D converter, which is mounted on the back side of the haptic hand and communicates to a main control PC with LAN. Therefore, high-precision force control was achieved while the number of wires in the control system was minimized.

This paper presents the design and specifications of a newly developed three-axis force sensor for the five-fingered haptic interface robot HIRO II+. The paper is organized as follows: In the next section, the mechanical design of HIRO II+ used here is summarized, and the newly developed control system for HIRO II+ is presented. In section 3, the design and specifications of the developed force sensor are presented, and then we consider the experiments of HIRO II+ with the developed force sensor and control system in section 4. The experimental results in free space and constraint space demonstrate the high potential of the five-fingered haptic interface robot equipped with the developed three-axis force sensors. Finally, section 5 presents our conclusions.

2. Five-fingered haptic interface

The authors have developed a five-fingered haptic interface, HIRO II+, consisting of a robot arm and a five-fingered haptic hand as shown in Fig. 1. HIRO II+ can present force and tactile feeling at the five fingertips of the human hand. First we introduce HIRO II+ briefly in subsection 2.1, and then we present the control system with the newly developed force sensor's amplifier circuit and interface FPGA circuit in subsection 2.2.

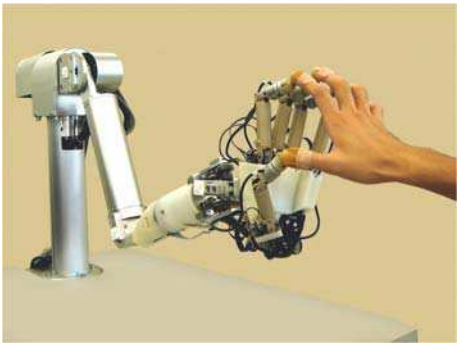

Fig. 1. Five-fingered Haptic Interface Robot: HIRO II+.

2.1 Mechanical design

Fig. 1 shows the five-fingered haptic interface HIRO II+ where it is coupled to the five fingers of an operator's hand. The haptic interface consists of an interface arm, a haptic hand with five haptic fingers, and a controller. When the operator moves his/her hand, the haptic interface follows the motion of the operator's fingertips and presents the sensation of force.

The operator feels only a small constriction because the only coupling between the human hand and the haptic interface occurs through the fingertips of the operator. The features of HIRO II+ are the following: (a) HIRO II+ can present force at the human five fingertips, (b) HIRO II+ can represent not only the force at the contact points but also the weight of virtual objects, (c) HIRO II+ should not cause an oppressive feeling when it is attached to humans and does not represent its own weight.

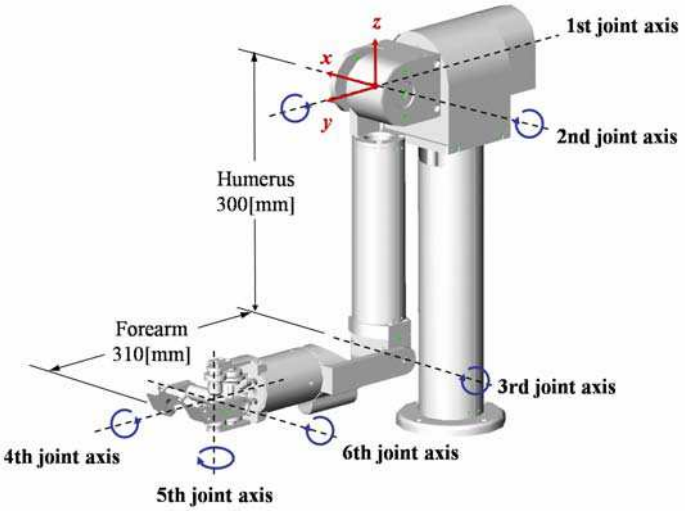

Fig. 2. Interface Arm design.

Degree of freedom	6	[dof]
Output force	45	[N]
Output moment	2.6	[Nm] (max)
Translational velocity	0.4	[m/s] (max)
Rotational velocity	1.4	[rad/s] (max)
Weight	6.9	[kgf]

Table 1. Specifications of the interface arm.

The interface arm is designed to be as close as possible to the human arm in geometry and motion ability, as shown in Fig. 2. The lengths of the upper arm and the forearm are 0.3 and 0.31 [m], respectively. The arm joints are actuated by AC servomotors equipped with rotary encoders and gear transmissions. The interface arm has 2 DOF at the shoulder joint, 1 DOF at the elbow joint, and 3 DOF at the wrist joint. The interface arm therefore has 6 joints allowing 6 DOF. Virtual work using the haptic interface can comfortably take place on the work space of a desktop. Table 1 shows the specifications of the interface arm.

The haptic hand starts from the wrist but does not include it, and ends at the fingertips. The hand base and five haptic fingers from the haptic hand are configured as shown in Fig. 3. The haptic fingers are designed to be similar to the human fingers in geometry and motion ability. Table 2 shows the specifications of the haptic hand. Each finger has 3 joints, allowing

3 DOF. The first joint, relative to the hand base, allows abduction/adduction. The second joint and the third joint allow flexion/extension. All joints are driven by DC servomotors with gear transmissions and rotary encoders. Another important issue in haptic finger design is the installation of the force sensors. In order to read the finger loading forces, a 6-axis force sensor (NANO sensor made by BL AUTOTEC, LTD.) in the second link of each finger is installed, of which 3-axis outputs, namely *x*-, *y*-, and *z*-elements, are used. The resolution of the force sensors F_x, F_y, and F_z, are 32, 32, and 98 [mN], respectively. Here, F_x, F_y, and F_z, are the *x*-, *y*-, and *z*-element output of the force sensor, respectively. To manipulate the haptic interface, the operator wears a finger holder on his/her fingertips as shown in Fig. 4. The finger holder has a sphere which, attached to the permanent magnet at the force sensor tip, forms a passive spherical joint. The role of the passive spherical joint attached by permanent magnet is to adjust the differences between the human and haptic fingers orientations and to ensure that the operator can remove his/her fingers from the haptic interface if it malfunctions. The suction force created by the permanent magnet is 5 [N].

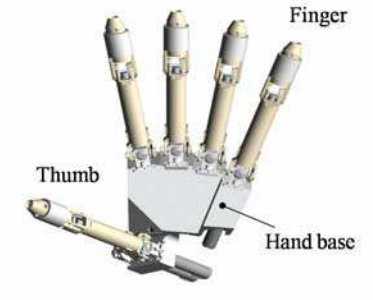

Fig. 3. Haptic hand design.

Hand	Number of fingers	5
	Degree of freedom	15 [dof]
	Weight	0.73 [kgf]
Finger	Degree of freedom	3 [dof]
	Output force	3.5 [N](max)
	Velocity	0.23 [m/s] (max)
	Weight	0.13 [kgf]

Table 2. Specifications of the haptic hand.

Fig. 4. Finger holder.

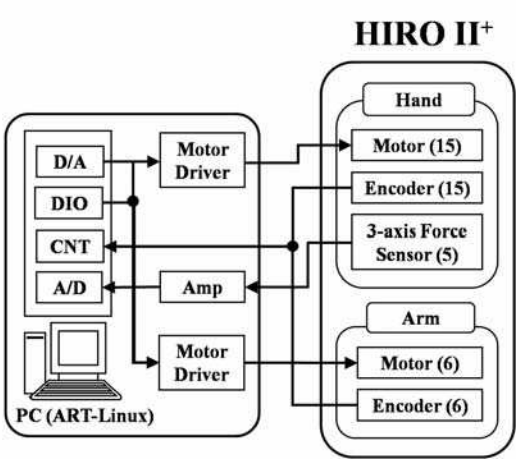

Fig. 5. Control system of HIRO II+.

The control system of HIRO II+ is shown in Fig. 5. The control system consists of a PC, a 12-bit digital-to-analogue converter (D/A), a 16-bit up/down counter (CNT), a 12-bit analogue-to-digital converter (A/D), digital input and output (DIO), a hand motor analogue power amplifier and an arm motor PWM driver. The real-time operating system ART-Linux is adopted to guarantee 1[ms] sampling time of the control.

2.2 Developed control system for haptic hand

Most haptic devices have a low reduction ratio, which permits impedance control without the use of a force sensor. However, this requires a large mechanism and entails difficulty in construction. The fact that the haptic finger of HIRO II+ uses a DC servomotor with a high reduction ratio ensures the compactness of the mechanism, but requires force sensors at the haptic fingertips. In particular, in order to accomplish high-precision force presentation to the operator, we need high-precision force sensors. On the other hand, in order to present the force at the five human fingertips, 15 DC servomotors and 5 force sensors are installed in the haptic hand of HIRO II+. Hence, the communication cable between the PC and haptic hand consists of 32 wires for the 15 encoders, 30 wires for the 15 DC servomotors, and 45 wires for the 5 force sensors, for a total wire count of 107. These wires greatly obstruct smooth movement of the haptic interface. Further, the amplifiers of the force sensors are stored under the haptic interface. Although the size of each force sensor amplifier is not large (each is 11×13×16 mm), many amplifiers are needed, and the total size becomes large. In order to solve these problems, we have developed high-precision force sensors and a compact sensor amplifier circuit with 15 channels. The force sensor signals are inputted to an interface FPGA circuit through a 24-bit A/D converter, which is mounted on the back side of the haptic hand and communicates to the main control PC with LAN. This leads to high-precision force control and reducing the number of wires of the control system. Next, we introduce the newly developed haptic hand control system, which consists of an interface FPGA circuit and a compact sensor amplifier circuit.

Fig. 6 shows the newly developed haptic hand control system made up of an interface FPGA circuit and a compact sensor amplifier circuit. The size of both circuits is 70×70 [mm], and

we can install these circuits on the back side of the haptic hand. The sensor amplifier circuit has a 24-bit A/D and 12-bit D/A converter. The five force sensors at the haptic fingertips are connected to the sensor amplifier circuit, and the output signals of the amplifier circuit are inputted to the interface FPGA circuit. The interface FPGA circuit and control PC are connected by Ethernet, so we could reduce the number of wires between the haptic hand and the control PC from 107 to 72: namely, 8 wires for Ethernet, 32 wires for the 15 encoders, 30 wires for the 15 DC servomotors and 2 wires for the power supply to the FPGA circuit. Furthermore, the sensor amplifier circuit has 15 channels. Hence the five force sensors can be covered by this one circuit. In the former system, we needed five amplifiers for the five force sensors. Although the size of each amplifier is not large, when five amplifiers are needed the total size becomes large: 190×105×150 [mm]. Therefore, by developing the sensor amplifier circuit, we could also miniaturize the total size of the haptic interface system.

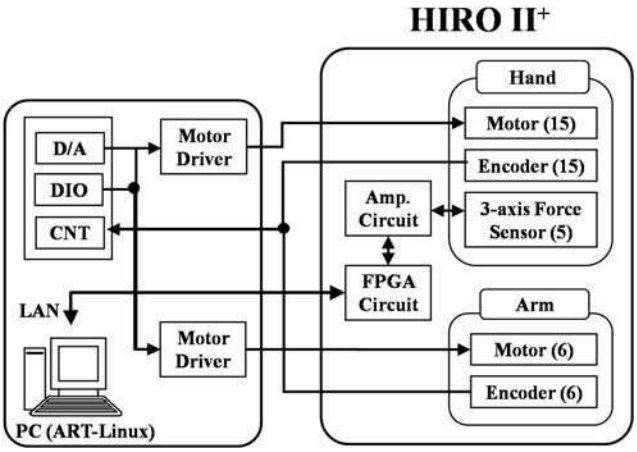

Fig. 6. Developed Control System.

Fig. 7. Interface FPGA circuit.

Fig. 7 shows the interface FPGA circuit, which has the following functions:

- Reading analogue voltages of the five force sensors
- Offset adjustment of voltages of the five force sensors
- Communication between the FPGA circuit and the control PC by UDP/IP

Table 3 shows the interface FPGA circuit specifications. In the FPGA chip, the digital signals of the force sensors from A/D are read, and FPGA sends these signals to the control PC each time the PC sends the commands. Moreover, when the PC sends the offset adjustment signals of the force sensors, FPGA sends digital signals corresponding to the offset adjustment signals to the D/A in the sensor amplifier circuit. As a result, the reading of the analogue voltages of the 5 force sensors and the offset adjustment of the voltages of the 5 force sensors are accomplished. The interface FPGA circuit is connected with the PC by Ethernet. The communication is fulfilled by UDP/IP, and is a command-and-response type communication. For the communication, we established several commands (Table 4).

Size	70×70×1.6 [mm]	
FPGA	Type	Xilinx Corp., Spartan3E(XCS500E)
	Clock frequency	100 [MHz]
Ethernet	Communication	100Base-TX
	Baud rate	100 [Mbps]
	protocol	UDP
Communication to sensor circuit	Serial communication specification	SPI (Serial Peripheral Interface)
	Communication clock frequency	2 [MHz]

Table 3. Specifications of the interface FPGA circuit.

Commands	Function
HiroHand_open_connection	Open connection between PC and FPGA by UDP/IP
HiroHand_close_connection	Close connection
HiroHand_force_offset	Offset adjustment of the force sensor
HiroHand_get_force	Measurement fingertips forces

Table 4. Examples of communication commands.

Fig. 8 shows the newly developed sensor amplifier circuit for the force sensors, and Table 5 shows the interface FPGA circuit specifications. The size of the circuits is 70×70×5 [mm], and the number of channels is 15. We installed a differential amplifier and low-pass filter in the amplifier output of the sensor amplifier circuit, and we gave 24-bit high resolution to the A/D converter in the sensor amplifier circuit. Thus, we consider that high-precision force

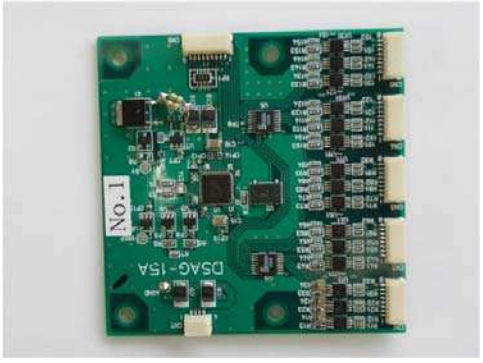

Fig. 8. Sensor amplifier circuit.

control, namely the reduction of the operational drag, is achieved. Further, we installed a 12 -bit D/A converter in the circuit because of the offset adjustment of the force sensors. The interface FPGA circuit and the sensor amplifier circuit are mounted on the back side of the haptic hand as shown in Fig. 9.

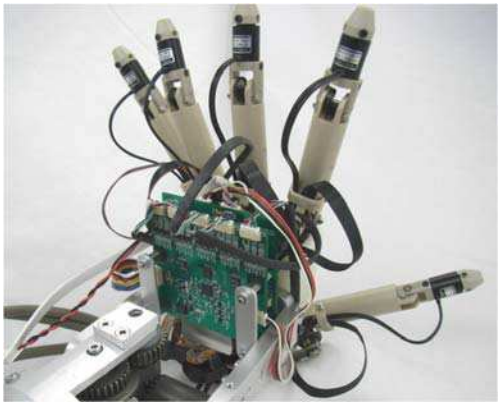

Fig. 9. Developed circuits installed in HIRO II+.

Channel number		15 (3ch×5)
bridge voltage		2.048 [v](all-channel common)
Amplifier output	differential amplifier	0~1.25~2.5 [V] with respect to the outputs of the force sensor -500~0~500 [με]
	low-pass filter	6 [dB/oct], Fc = 100 [Hz]
A/D converter	Type	ADS1258 (Texas Instruments Inc)
	resolution	24 [bit]
	channel	16 (we used 15ch)
D/A converter	Type	AD5328 (Analog Devices Inc)
	Adjustment	By using 0~1.25~2.5[V], -500~0~500[με] can be adjustment.
	Resolution	12 [bit]
	channel	16 (we used 15ch: 8ch×2)
Power supply		DC 5[V](0.5[A]) and DC3.3[V](0.1[A])
Size		W70×D70×H5 [mm]

Table 5. Specifications of the sensor amplifier circuit.

3. Three-axis force sensor

3.1 Design concept and specifications

The purpose of the developed force sensor is to measure the three-axis forces, F_x, F_y, and F_z, at the haptic fingertip. Unlike most haptic devices that have a low reduction ratio, HIRO II+ uses a DC servomotor with a high reduction ratio. A high-precision force sensor is required to accomplish high-precision force presentation. The force sensor is installed in the second link of each haptic finger and is connected to the developed sensor amplifier circuit, introduced in subsection 2.2. The size of the force sensor has to be small enough to install at the haptic fingertip. We set the following development goals for the force sensor:

- Low load $F_x = F_y = F_z$ =10 [mN] can be measured;
- The outside diameter is 14 [mm]; and
- The interference between each axis force in the sensor element is minimal.

Fig. 10 shows the newly developed three-axis force sensor, and Fig. 11 shows its dimensional outline drawing. By using the strain gauge in the pressure port of the sensor element, the force sensor measures the force from the deformation of the metal beam. The force sensor with strain gauge has the following advantages:

- The sensor has better linearity;
- The sensor has a small effect of temperature change; and
- The force sensor is suitable for the measurement of dynamic phenomena because the amount of the displacement is extremely small.

In order to accomplish the development goals, we need a sensor element that can measure the three axes forces with accuracy in a tight space.

Fig. 10 Three-axis force sensor.

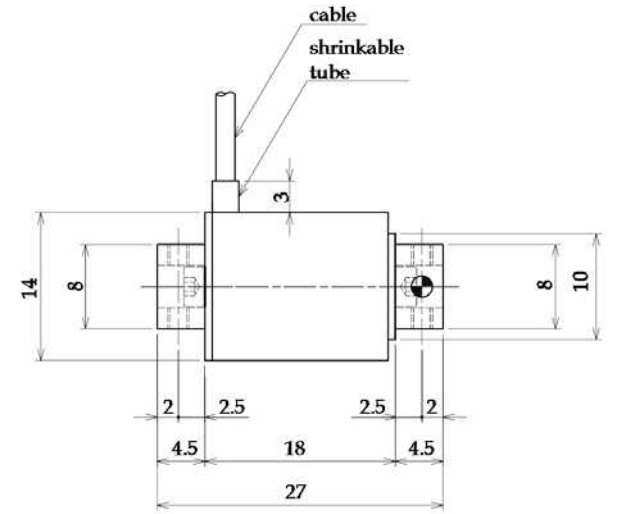

Fig. 11 The dimensional drawing of the force sensor.

3.2 Sensor structure

Fig. 12 shows the sensor structure of the developed three-axis force sensor. For the acting axis force, the strain gauges are installed at the surface of the spot where the stress of the sensor element reaches a maximum, and the force is detected as the change in electrical resistance. The total number of strain gauges is 16: x1~x4, y1~y4, and z1~z8. For the forces in the X- and Y-directions, the bending strains of x1~x4 and y1~y4 are detected, respectively. Further, the shear strains of z1~z8 are detected for the force in the Z-direction. Fig. 13 shows the circuit of the strain gauges. For each pair of strain gauges which detect the corresponding axis force, a Wheatstone bridge is applied. In order to simplify the wire system, the power supply to the bridge circuits is common, and we set up 8: 2 wires for the input (power supply to bridge) and 6 wires for the output (F_x-output, F_y-output, and F_z-output). The output of the circuit is expressed as the strain [$\times 10^{-6}$], and the force is measured by calibrating the relation between the load and the strain.

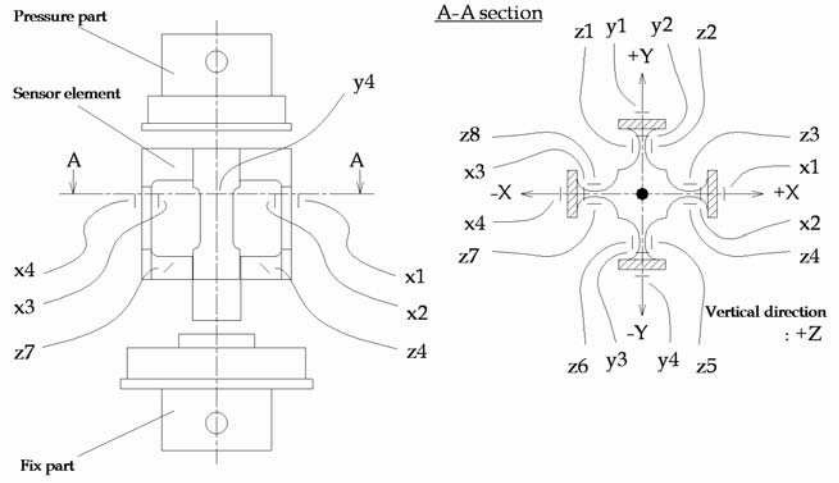

Fig. 12 Force sensor structure.

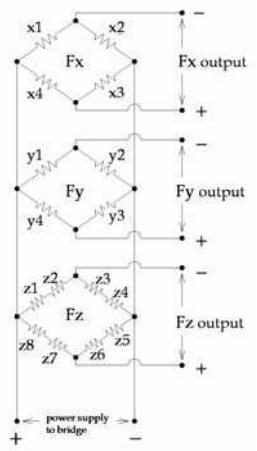

Fig. 13 Bridge circuit.

3.3 Basic characteristics

Fig. 14 shows the three-axis forces of the force sensor. From the calibration tests, we could obtain the relationship between the load and the strain in each axis direction as shown in Figs. 15, 16, and 17. The basic characteristics of the developed three-axis force sensor are the following: The rated load is 10 [N]. For the rated load, the rated outputs of the X-direction, Y-direction, and Z-direction are $\varepsilon x=1300\times10^{-6}$, $\varepsilon y=1300\times10^{-6}$, and $\varepsilon z=350\times10^{-6}$, respectively, where ε^* is the strain of the *-direction. Nonlinearity and hysteresis, which reflect the performance of the force sensor, are about 0.3%RO (Rated Output). Therefore, it can be said that the output strain is linear with respect to the load in each axis direction. Further, the interference output between each axis force also has linearity. Hence, the acting force can be derived by correcting the mutual interference. Table 6 shows the specifications of the developed three-axis force sensor.

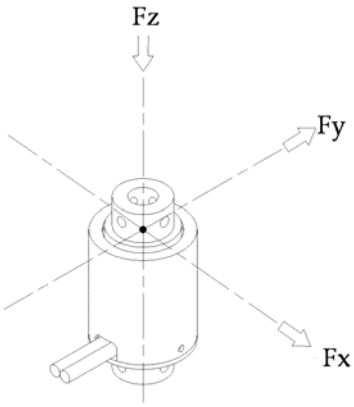

Fig. 14. Three axis forces.

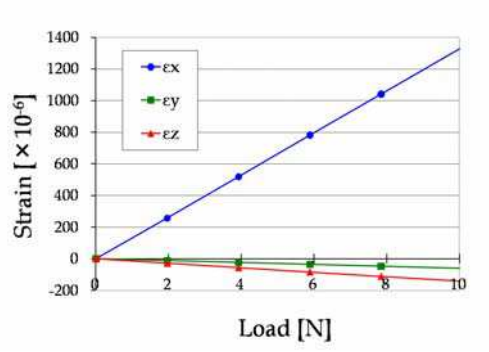

Fig. 15. Strain output w.r.t. the load in the +X direction.

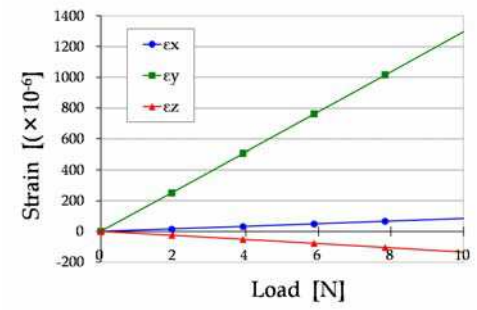

Fig. 16. Strain output w.r.t. the load in the +Y direction.

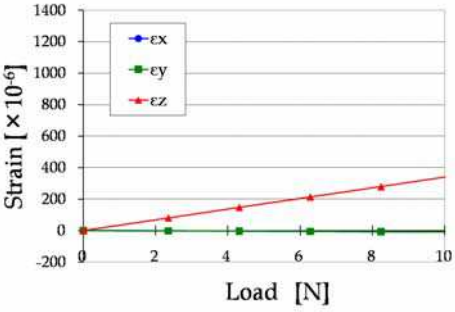

Fig. 17. Strain output w.r.t. the load in the +Z direction.

Rated capacity		10	[N]
Rated output	X-, Y-direction	±0.5	[mV/V] (±1000×10-6 strain)
	Z-direction	±0.15	[mV/V] (±300×10-6 strain)
Safe overload		200	[%]
Nonlinearity		≤ |1.0|	[%RO]
Hysteresis		≤ |1.0|	[%RO]
Repeatability		≤ 1.0	[%RO]
Safe temperature range		10~70	[˚C]
Temperature effect on zero	X-, Y-direction	±0.05	[%RO/˚C]
	Z-direction	±0.10	[%RO/˚C]
Temperature effect on output	X-, Y-direction	±0.05	[%RO/˚C]
	Z-direction	±0.10	[%RO/˚C]
Input-output resistance	input	48±5%	[Ω]
	X-, Y-output	120±5%	[Ω]
	Z-output	240±5%	[Ω]
Weight		14.7	[g]

Table 6. Specifications of the developed force sensor.

4. Experiment of haptic interface using three-axis force sensor

In order to evaluate the developed three-axis force sensor, including the compact sensor amplifier circuit and the interface FPGA circuit, we carried out two kinds of experiments. One was the manipulation of the haptic interface in free space, and the other was the manipulation of the haptic interface in constraint space. In each experiment, we compared the experimental results of HIRO II+ with the developed force sensor and HIRO II+ with the former force sensor. Figs. 5 and 6 show the control system of the HIRO II+ with the developed force sensor and HIRO II+ with the former force sensor, respectively. As the control law of the haptic interface, we used the following redundant force control: The control of the haptic hand is given by

$$\tau(t) = J^T \left\{ K_1 F_e(t) + K_2 \int_0^t F_e(s)ds + F_d \right\} - K_3 \dot{q}_f(t) \tag{1}$$

where $\tau \in R^{15}$ is a joint torque vector of each finger of the haptic hand, $J \in R^{15\times 15}$ is a kinematic Jacobian, $F = [F_1^T, F_2^T, \cdots, F_5^T]^T \in R^{15}$ is a force vector whose sub vector is the force vector at the fingertip, $F_d = [F_{d1}^T, F_{d2}^T, \cdots, F_{d5}^T]^T \in R^{15}$ is the desired force, $F_e = F_d - F$, and $q_f = [q_1^T, q_2^T, \cdots, q_5^T]^T \in R^{15}$ is a joint angle vector of the haptic finger. Further, $K_i \in R^+$ is the feedback gain matrix. On the other hand, the control of the interface arm is given by

$$\tau_a(t) = K_{a1}\tau_e(t) + K_{a2}\int_0^t \tau_e(s)ds - K_{a3}\dot{q}_f(t) + J_a^T \begin{pmatrix} \sum_{i=1}^{k} F_{di} \\ \sum_{i=1}^{k} (p_i - p_{hb}) \times F_{di} \end{pmatrix} \tag{2}$$

where $K_{ai} \in R^+$ is the feedback gain matrix, $q_{fa} = [q_{a1}, q_{a2}, \cdots, q_{a6}]^T$ is the joint angle vector, $J_a \in R^{6\times 6}$ is a kinematic Jacobian, $p_i \in R^3$ is the *i*-th fingertip position vector, $p_{hb} \in R^3$ is the tip of the interface arm and

$$\tau_e(t) = J_a^T \begin{pmatrix} \sum_{i=1}^{5} (F_{di} - F_i) \\ \sum_{i=1}^{5} (p_i - p_{hb}) \times (F_{di} - F_i) \end{pmatrix}$$

is an equivalent joint torque to the offset forces $(F_{di} - F_i)$ at the five fingertips. Details of the control law have been shown in (Kawasaki & Mouri, 2007). On the other hand, the control PC uses a real-time OS (ART-Linux) to guarantee 1 [ms] sampling time, for the experiments.

4.1 Manipulation in free space

Fig. 18 shows the responses of HIRO II+ with the developed force sensor in free space, and Fig. 19 shows the responses of HIRO II+ with the former force sensor in free space. In each figure, (a) shows the responses of the five fingertip positions and (b) shows the responses of the five fingertip forces. Note that we considered the following force error for the *i*-th fingertip's force error: $F_e^i = \sqrt{F_x^2 + F_y^2 + F_z^2}$. In both cases, the five fingers of the operator

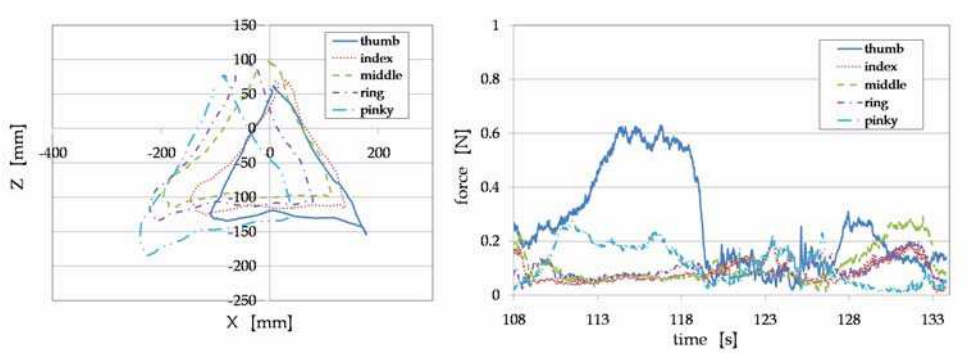

(a) fingertip positions (b) fingertip forces

Fig. 18. Responses of HIRO II+ with developed force sensor in free space.

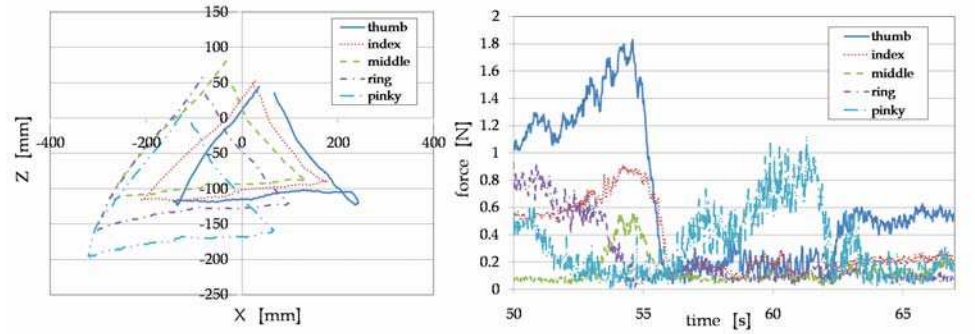

(a) fingertip positions (b) fingertip forces

Fig. 19. Responses of HIRO II+ with former force sensor in free space.

are connected to the haptic interface, and the operator moved his five fingertips like drawing triangle. In the experiment, we considered the manipulation of the haptic interface

in free space. Hence, the desired forces at the five fingertips are set to zero. But, the responses of the fingertip forces have a slight force error. In order to consider the force error quantitatively, we considered the average force error. The average force errors of HIRO II+ with the developed force sensor and HIRO II+ with the former force sensor were 0.13 [N] and 0.33 [N], respectively. The responses of HIRO II+ with the developed force sensor in free space were apparently improved. However, in contrast with the finger joints' backlash and the friction, those of the arm joints are large, and we have considered that a large part of the above average force error 0.13 [N] was caused by the interface arm.

4.2 Manipulation in constrained space

Next, we considered the manipulation of the haptic interface in constraint space. In the experiment, the five fingers of the operator are connected to the haptic interface, and the operator moved his five fingertips like drawing triangle while grasping the cube in the VR space as shown in Fig. 20.

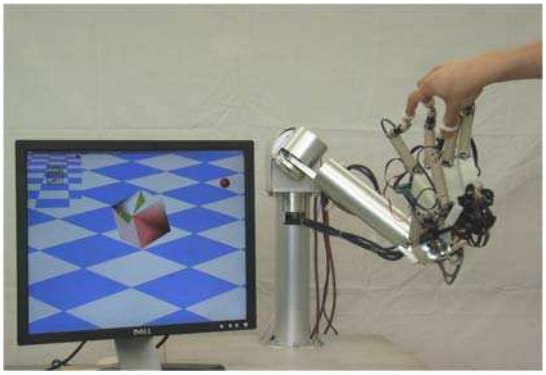

Fig. 20. Experimental environment.

Fig. 21 shows the responses of HIRO II+ with the developed force sensor in the constraint space, and Fig. 22 shows the responses of HIRO II+ with the former force sensor in the constraint space. In each figure, (a) shows the responses of the five fingertip positions and

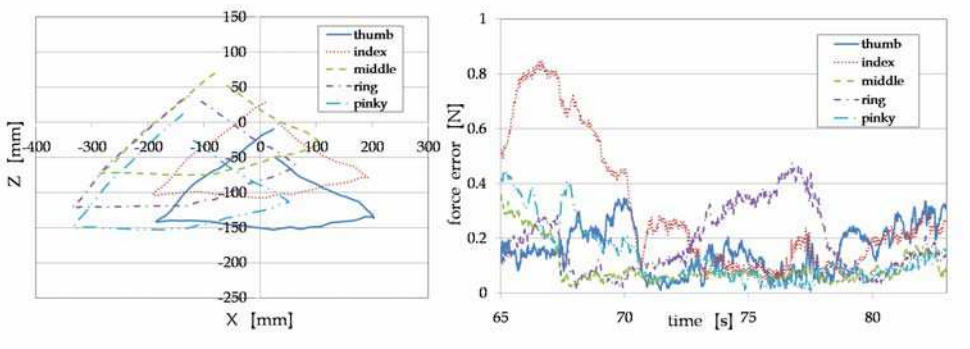

(a) fingertip positions (b) fingertip force errors

Fig. 21. Responses of HIRO II+ with developed force sensor in constraint space.

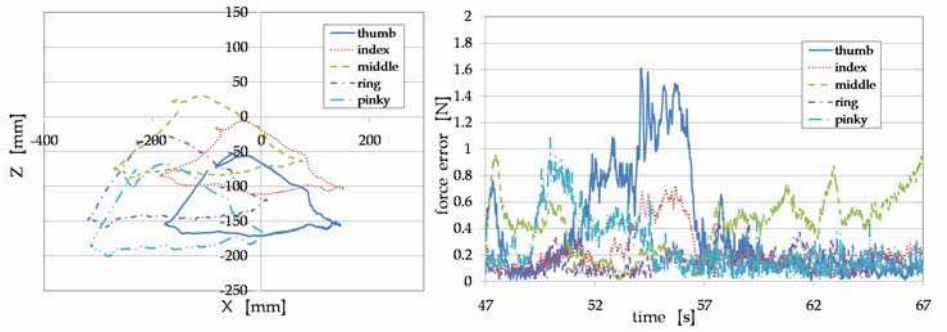

(a) fingertip positions (b) fingertip force errors

Fig. 22. Responses of HIRO II+ with former force sensor in constraint space.

(b) shows the responses of the five fingertip force errors. The following equation was used for the *i*-th fingertip's force error: $F_e^i = \sqrt{(F_x - F_x^d)^2 + (F_y - F_y^d)^2 + (F_z - F_z^d)^2}$. The desired force at each finger was set to be $F_i^d = Kx_i + D\dot{x}_i$, where x_i is the penetration depth of the *i*-th finger into the cube, K (=600[N/m]) is the stiffness of the cube, and D (=1.0×10-4[Ns/m]) is the damping coeeficient of the cube. The average force errors of HIRO II+ with the developed force sensor and HIRO II+ with the former force sensor were 0.17 [N] and 0.28 [N], respectively. The responses of HIRO II+ with the developed force sensor in the constraint space were apparently improved. However the responses of the fingertip forces have a slight force error.

We have considered that the resolution of the force sensors, characteristics of the motor amplifiers, adjustments of the feedback gain in the control law, and the backlash and friction in the mechanism are related to the existing slight force error. In this study, we mainly considered the resolution of the force sensor. In order to develop a better haptic interface, we must clarify the cause and plan to investigate these problems as challenges for the future.

5. Conclusion

In this paper, we have developed a small size high-precision three-axis force sensor, a compact sensor amplifier circuit with 24-bit high resolution, and an interface FPGA circuit. These circuits are mounted on the back of the haptic hand, and the output signals of the force sensors are input to the interface FPGA circuit, which communicate to the main control PC with LAN. Therefore, we could reduce the number of wires in the control system. Furthermore, we carried out an experimental test and confirmed the improvement of the haptic interface. This experiment demonstrates the high potential of the five-fingered haptic interface robot HIRO II+ with the developed three-axis force sensors. The next problem to be tackled is to investigate the cause of the force error and based on those results, to improve HIRO II+ further. This paper was supported by the Ministry of Internal Affairs and Communications Strategic Information and Communications R&D Promotion Programme (SCOPE) and by a JSPS Grant-in-Aid for Scientific Research (B) (19360190).

6. References

Adachi, Y.; Kumano, T.; Ikemoto, A.; Hattori, A. & Suzuki, N. (2002). Development of a haptic device for multi fingers by macro-micro structure. (in Japanese) *J. Robot. Soc. Jpn.,* Vol.20, No.7, pp. 725-733

Ando, N.; Korondi, P, T & Hashimoto, H. (2001). Development of Micromanipulator and Haptic Interface for Networked Micromanipulation. *IEEE/ASME Trans. Mechatron.,* Vol.5, No.2, pp. 417-427

Basdogan, C.; Ho, C. & Srinivasan, M. (2001). Virtual Environments for Medical Training: Graphical and Haptic Simulation of Laparoscopic Commom Bile Duct Exploration. *IEEE/ASME Trans. Mechatron.,* Vol.6, No.3, pp. 269-286

Bouzit, M.; Burdea, G.; Popescu, G. & Boian, R. (2002). The Rutgers Masster II - New Design Force-Feed backGlove. *IEEE/ASME Trans. Mechatron.,* Vol.7, No.2, pp. 256-263

Elhajj, I.; Xi, N; Fung; W.; Liu, Y; Li, W; Kaga, T & Fukuda, T. (2001). Haptic Information in Internet-Based Teleoperation. *IEEE/ASME Trans. Mechatron.,* Vol.6, No.4, pp. 295-304

Immersion Corporation. CyberForce [Online]. Available: http://www.immersion.com/

Ivanisevic, I. & Lumelsky, V. (2000). Configuration Space as a Means for Augmenting Human Performance in Teleoperation Tasks. *IEEE Trans. Syst., Man Cybern. B,* Vol.30, No.3, pp. 471-484

Kawasaki, H. & Hayashi, T. (1993). Force Feedback Glove for Manipulation of Virtual Objects. *J. of Robotics and Mechatronics,* Vol.5, No.1, pp. 79-84

Kawasaki, H. ; Takai, J. ; Tanaka, Y. ; Mrad, C. & Mouri, T. (2003). Control of multi-fingered haptic interface opposite to human hand, *Proceedings of IROS 2003*, pp. 2707-2712, Nevada, USA, October, 2003

Kawasaki, H. & Mouri, T. (2007). Design and control of five-fingered haptic interface opposite to human hand. *IEEE Trans. on Robotics,* Vol.23, No.5, pp. 909-918

Langrana, N.; Burdea, G.; Lange, K.; Gomez, D. & Deshpande, S. (1994). Dynamic force feedback in a virtual knee palpation. *Artif. Intell. Med.,* Vol.6, pp. 321-333

Magnenat-Thalmann, N & Bonanni, U. (2006). Haptics in virtual reality and multimmedia. *IEEE Multimedia*, Vol.13, No.3, pp. 6-11

Ueda, Y. & Maeno, T. (2004). Development of a Mouse-Shaped Haptic Device with Multiple Finger Inputs, *Proceedings of IROS 2004*, pp. 2886-2891, Sendai, Japan, 2004

Walairacht, S.; Ishii, M.; Koike. Y. & Sato, M. (2001). Two-Handed Multi-Fingers String-basesd Haptic Interface Device. *IEICE Trans. On Information and Systems*, E84D, No.3, pp. 365-373

Yoshikawa, T. & Nagara, A. (2000). Development and control of touch and force display devices for haptic interface, *Proceedings of SYROCO 2000*, pp. 427-432, Vienna, Austria, September, 2000

Sensors: Focus on Tactile Force and Stress Sensors

Edited by Jose Gerardo Rocha and Senentxu Lanceros-Mendez

ISBN 978-953-7619-31-2
Hard cover, 444 pages
Publisher InTech
Published online 01, December, 2008
Published in print edition December, 2008

This book describes some devices that are commonly identified as tactile or force sensors. This is achieved with different degrees of detail, in a unique and actual resource, through the description of different approaches to this type of sensors. Understanding the design and the working principles of the sensors described here requires a multidisciplinary background of electrical engineering, mechanical engineering, physics, biology, etc. An attempt has been made to place side by side the most pertinent information in order to reach a more productive reading not only for professionals dedicated to the design of tactile sensors, but also for all other sensor users, as for example, in the field of robotics. The latest technologies presented in this book are more focused on information readout and processing: as new materials, micro and sub-micro sensors are available, wireless transmission and processing of the sensorial information, as well as some innovative methodologies for obtaining and interpreting tactile information are also strongly evolving.

INTECH
open science | open minds

InTech Europe
University Campus STeP Ri
Slavka Krautzeka 83/A
51000 Rijeka, Croatia
Phone: +385 (51) 770 447
Fax: +385 (51) 686 166
www.intechopen.com

InTech China
Unit 405, Office Block, Hotel Equatorial Shanghai
No.65, Yan An Road (West), Shanghai, 200040, China
中国上海市延安西路65号上海国际贵都大饭店办公楼405单元
Phone: +86-21-62489820
Fax: +86-21-62489821